HHS Public Access

Author manuscript

Oncogene. Author manuscript; available in PMC 2014 February 15.

Published in final edited form as:

Oncogene. 2013 August 15; 32(33): 3867–3876. doi:10.1038/onc.2012.394.

AGR2 is a SMAD4-suppressible gene that modulates MUC1 levels and promotes the initiation and progression of pancreatic intraepithelial neoplasia

A.M. Norris[1], **A. Gore**[4], **A. Balboni**[2], **A. Young**[1], **D.S. Longnecker**[3], and **M. Korc**[4,†]

[1]Department of Medicine, Dartmouth Medical School, Hanover, NH 03755, USA

[2]Department of Pharmacology and Toxicology, Dartmouth Medical School, Hanover, NH 03755, USA

[3]Department of Pathology, Dartmouth Medical School, Hanover, NH, 03755, USA

[4]Departments of Medicine, Biochemistry and Molecular Biology, Indiana University School of Medicine, the Melvin and Bren Simon Cancer Center, and the Pancreatic Cancer Signature Center, Indianapolis, IN 46202, USA

Abstract

The mechanisms controlling expression of the putative oncogene AGR2 in pancreatic ductal adenocarcinoma (PDAC) are not well understood. We now show that AGR2 is a TGF-β-responsive gene in human pancreatic cancer cells, whose down-regulation is SMAD4-dependent. We also provide evidence supporting a role for AGR2 as an ER-chaperone for the cancer-associated mucin, MUC1. AGR2 is both sufficient and required for MUC1 expression in pancreatic cancer cells. Furthermore, AGR2 is co-expressed with MUC1 in mouse pancreatic intraepithelial neoplasia (mPanIN)-like lesions and in the cancer cells of four distinct genetically engineered mouse models of PDAC. We also show that *Pdx1-Cre/LSL-Kras*^{G12D}*/Smad4*$^{lox/lox}$ mice heterozygous for *Agr2* exhibit a delay in mPanIN initiation and progression to PDAC. It is proposed that loss of *Smad4* may convert TGF-β from a tumor suppressor to a tumor promoter by causing the up-regulation of AGR2, which then leads to increased MUC1 expression, at which point both AGR2 and MUC1 facilitate mPanIN initiation and progression to PDAC.

Keywords

TGF-β; AGR2; pancreatic cancer; MUC1; SMAD4

†Corresponding author: Murray Korc, M.D., Indiana University School of Medicine, 980 West Walnut Street, Indianapolis, IN 46202, Phone: 317-278-6410, Fax: 317-274-8046, mkorc@iupui.edu.

Conflict of Interest

The authors have no conflicts of interest to disclose.

Supplementary information is available on Oncogene's website.

Introduction

Pancreatic ductal adenocarcinoma (PDAC) is a deadly malignancy with a median survival of six months and five-year survival rates of 6% [1]. PDAC is characterized by multiple molecular alterations that include mutations in the *K-ras* oncogene, and the *p53*, *p16*, and *SMAD4* tumor suppressor genes occurring in conjunction with overexpression of tyrosine kinase receptors and transforming growth factor-β (TGF-β) isoforms [2-5].

TGF-βs act as tumor suppressors and inhibit the proliferation of epithelial cell types [5]. However, pancreatic cancer cells are of epithelial origin and are generally resistant to TGF-β-mediated growth inhibition, due to the presence of *SMAD4* mutations or deletions [6], the under-expression of the type I TGF-β receptor (TβRI; [7, 8]), and/or the overexpression of inhibitory SMAD6 or SMAD7 [9, 10]. Moreover, increased expression of TGF-βs in PDAC is associated with decreased patient survival [11] and, under certain culture conditions, TGF-βs stimulate pancreatic cancer cell growth [12]. Thus, TGF-βs contribute to the biological aggressiveness of PDAC through a variety of mechanisms.

PDAC is also characterized by the presence of an abundant stroma and increased production of mucins [13]. Three mucins in particular have been associated with more rapid disease progression in PDAC: MUC1, MUC4, and MUC5AC [14-18]. Both MUC1 and MUC4 are directly implicated in cancer progression and metastasis, through their effects on cell-to-cell signaling [19] and as a consequence of their ability to activate EGFR [20, 21] and/or HER2 pathways [22].

Anterior gradient 2 (AGR2) is a secreted protein that contains an endoplasmic reticulum (ER) leader sequence [23]. It is a potential member of the ER-associated protein disulfide isomerase (PDI) family as evidenced by its structural similarity to PDI proteins [24-26], and it forms mixed disulfide bonds with the intestinal mucin protein MUC2 [25]. AGR2 expression in tumors appears to depend on the tissue of origin [27-34], is elevated in a number of adenocarcinomas [23, 27, 35-38], and confers a metastatic phenotype when overexpressed *in vitro* [27, 39]. In PDAC, AGR2 promotes cancer cell dissemination by enhancing the expression of lyosomal proteases [38], and by increasing cancer cell survival and chemoresistance [40].

In the present study, we sought to further delineate the role of AGR2 in PDAC. We now report that AGR2 is downregulated by TGF-β in a SMAD4-dependent manner and that AGR2 acts as an ER-localized molecular chaperone of MUC1 in pancreatic cancer cells, co-localizes with MUC1 in pancreatic lesions *in vivo*, and is essential for MUC1 expression. We also show that *Pdx-1-Cre*/*LSL-Kras*^{G12D}/*Smad4*$^{lox/lox}$ mice null for *Agr2* exhibit decreased formation of mouse pancreatic intraepithelial neoplasia (mPanIN)-like lesions and attenuated progression to PDAC.

Results

AGR2 expression is regulated by TGF-β

AGR2 was identified as a TGF-β1 down-regulated gene as part of an effort in our laboratory to discover novel TGF-β responsive genes in PDAC [10, 41]. To better characterize the interactions between TGF-β1 signaling and AGR2, we studied the effects of TGF-β1 on AGR2 mRNA and protein levels in four human pancreatic cancer cell lines (Fig. 1). TGF-β1 markedly decreased AGR2 mRNA levels in COLO-357 and PANC-1 cells, but had not in ASPC-1 or BxPC3 cells (Fig. 1A). TGF-β1-mediated inhibition of AGR2 mRNA levels in PANC-1 and COLO-357 cells was evident as early as three hours in COLO-357, and was maximal in both cell lines at 24 hours (Fig. 1B). It was preceded by a slight, transient and statistically insignificant increase in AGR2 mRNA levels at 3 hours in PANC-1 cells, (Fig. 1B). A luciferase assay was therefore carried out to assess the response of the AGR2 promoter to TGF-β in these cells. It demonstrated that TGF-β1 decreased AGR2 transcriptional activity in PANC-1 cells even at this early time point (Fig. S1), raising the possibility that in these cells TGF-β1 induced a slight early increase in AGR2 mRNA stability.

TGF-β1 also decreased AGR2 protein levels in COLO-357 and PANC-1 cells, but not in ASPC-1 and BxPC3 cells (Fig. 1C-D). A decrease in AGR2 protein could be detected as early as 16 hours following TGF-β1 addition in both cell lines and was maximal at 48 hours (Fig. 1E-F). After confirming antibody specificity (Fig. S2), we determined that this effect was consistent regardless of the concentration of serum used (Fig. S3).

AGR2 expression is regulated by SMAD4

ASPC-1 cells harbor a mutated SMAD4, whereas BxPC3 cells are devoid of SMAD4 due to a homozygous deletion of the gene [6, 42]. By contrast, COLO-357 cells and PANC-1 cells express wild type SMAD4 [43]. Inasmuch as SMAD4 is a key effector for canonical TGF-β signaling [6, 44, 45], we next sought to determine the consequence of restoring wild-type SMAD4 on AGR2 expression. TGF-β1 reduced AGR2 mRNA levels in cells expressing wild-type SMAD4 (COLO-357 and PANC-1), but not in cells with mutated or absent SMAD4 (ASPC-1 and BxPC-3; Fig. 1 and 2A). In these cells, however, restoration of SMAD4, irrespective of the absence or presence of TGF-β1, caused a significant decrease in AGR2 mRNA (Fig. 2A).

To determine whether SMAD4 was required for the TGF-β1-mediated decrease in AGR2 mRNA levels, COLO-357 cells were stably transfected with the pGIPZ-S4 construct to induce stable SMAD4 knockdown (Fig. 2B). Suppression of endogenous SMAD4 resulted in increased AGR2 mRNA (not shown) and protein levels (Fig. 2B), which were no longer modulated by TGF-β1. By contrast, stable transfection of COLO-357 cells with pGIPZ-scr (scrambled control) did not alter endogenous AGR2 protein levels, which were again reduced by TGF-β1 (Fig. 2B).

Attempts to perform chromatin immunoprecipitation (ChIP) assays to determine whether AGR2 is a transcriptional target of SMAD4 were not successful, likely due to the complicated mechanisms of SMAD4 transcriptional signaling [46], a nd the potentially low

DNA binding affinity of SMAD4 in pancreatic cancer cells. Therefore, the 5′UTR of *AGR2* was screened for established SMAD4 binding CAGA boxes [45, 47]. Previous studies have demonstrated *AGR2* responsive reporters using up to −1.7 kb base pairs of the 5′UTR [30, 48]. Two putative SMAD binding elements (SBEs) were located within this region: 5′-*CACAGACAG*-3′ at −1535 bp and 5′-*TGCAGACCT*-3′ at −773 bp. An AGR2 promoter reporter (*AGR2*-luc) was cloned by placing −2595 bp of the *AGR2* 5′UTR upstream from the luciferase gene in the *pGL3* vector (Fig. S4A). Constructs containing a point mutation in one or both of the SBEs in *AGR2*-luc were also generated.

To confirm that transfection of exogenous SMAD4 (by *pCMV5-DPC4-HA*; [49]) was sufficient to activate SMAD transcriptional activity, we used the SMAD-responsive luciferase reporter construct *SBE4*-luc [50]. *SBE4*-luc was induced three fold in a luciferase assay after expression of SMAD4 alone (Fig. S4B). We next determined the effects of SMAD4 expression on AGR2 promoter activity and found that SMAD4 reduced *AGR2* promoter luciferase activity two fold (Fig. 2C). Furthermore, if either or both of the SBEs were mutated, SMAD4 had no effect on *AGR2*-luc (Fig. 2C), suggesting that both of these sites are important for SMAD4-mediated repression of AGR2.

AGR2 is localized to the endoplasmic reticulum of pancreatic cancer cells

AGR2 is associated with the endoplasmic reticulum (ER) of intestinal cells [25, 26]. To determine whether AGR2 localized to the ER in pancreatic cancer cells, immunofluorescence (IF) was performed in PANC-1 cells in relation to AGR2 (Fig. 3A, red) and the ER-associated chaperone GRP78 (Fig. 3A, green). The merged image revealed that they were co-localized, particularly in the peri-nuclear space (Fig. 3A). Moreover, live-cell confocal microscopy on PANC-1 cells expressing a fusion AGR2-RFP protein and stained with an ER-tracker dye (Fig. 3B) confirmed that AGR2 localizes mostly to the ER.

AGR2 interacts with and is required for MUC1 expression

Mucins are large proteins that require extensive folding in the ER [51]. AGR2 was shown to be essential for the production of intestinal-associated mucin, MUC2 [25]. We therefore sought to determine whether AGR2 is also associated with the pancreatic-expressed mucin, MUC1. By IF, AGR2 co-localized with MUC1 in PANC-1 cells, both in the cytoplasm and in the peri-nuclear space (Fig. 4A). Tight co-localization patterns were also observed in COLO-357 and BxPC3 (*SMAD4* deficient) cells (Fig. S5). Moreover, co-immunoprecipitation (co-IP) experiments revealed that MUC1, but not MUC4 or MUC5AC, immunoprecipitated with AGR2 (Fig. 4B).

To determine whether AGR2 was required for MUC1 expression, COLO-357 cells, which express high endogenous levels of AGR2, were transfected to stably express a doxycycline (DOX)-inducible shRNA that targets AGR2 (pTRIPZ-AGR2), or a negative control (pTRIPZ-scramble). After incubation with increasing concentrations of DOX, there was a dose-dependent decrease in both AGR2 mRNA (Fig. 4C) and protein (Fig. 4D) levels in the pTRIPZ-AGR2 clones, which was associated with a dose-dependent reduction in MUC1 protein levels (Fig. 4D), but not MUC1 mRNA levels (not shown). In agreement with previous findings [26], AGR2 silencing in COLO-357 cells created an ER stress response

after 48 and 72 hours, as evidenced by increased phosphorylation of eIF2α and PERK (Fig. S6).

To determine whether the consequences of AGR2 knockdown on MUC1 protein were reversible, we performed a rescue experiment using mouse AGR2 (mAGR2). To first confirm that the pTRIPZ-AGR2 silencing vector did not target mAGR2, cells were transfected with a mAGR2 expression construct (pcDNA-mAGR2), or an empty pcDNA vector. AGR2 and mAGR2 mRNA levels were then measured in sham and mAGR2 transfected populations, either with or without simultaneous activation of the AGR2 silencing vector (Fig. 4E). As expected, endogenous AGR2 levels were not significantly affected by the transfection of mAGR2, but were diminished about 80% by DOX. Conversely, following pcDNA-mAGR2 transfection, mAGR2 was increased and was not reduced by the silencing vector.

We next determined whether rescuing AGR2 knockdown with mAGR2 would prevent the associated decrease in MUC1 protein levels. AGR2 knockdown was again associated with reduced MUC1 protein levels (Fig. 4F), which was not due to a non-specific effect on MUC genes, as MUC4 levels were not reduced. However, mAGR2 expression prevented AGR2 silencing from altering MUC1 protein levels (Fig. 4F), suggesting that the decrease of MUC1 after AGR2 silencing is specific and reversible. We next sought to determine whether TGF-β1 modulated MUC1 expression. Similar to the pattern of AGR2 inhibition by TGF-β1 (Fig. 1), MUC1 levels were decreased, but only in the SMAD4-proficient COLO-357 and PANC-1 cells and not in the BxPC-3 cells (ASPC-1 cells did not express MUC1 RNA or protein; Fig. 4H). Of note, MUC1 immunoblots revealed the presence of two bands in PANC-1 cells, suggesting that MUC1 undergoes protein modification or differential folding in these cells.

Inasmuch as AGR2 and MUC1 expression is elevated in PDAC, we next determined if AGR2 overexpression was sufficient to induce MUC1. Since AGR2 protein levels were lowest in PANC-1 cells, we created stable PANC-1 clones expressing either an empty pcDNA vector (sham) or a pcDNA-AGR2 expression plasmid. PANC-1 cells that overexpressed AGR2 also had elevated MUC1 levels (Fig. 4G), suggesting that AGR2 expression is sufficient to stabilize MUC1 expression.

AGR2 is associated with MUC1 expression in pancreatic lesions

To determine whether AGR2 and MUC1 were associated in pancreatic lesions *in vivo*, MUC1 and AGR2 expression was examined by IF in four genetically engineered mouse models (GEMMs) of PDAC: *Pdx1-Cre/Kras*^{G12D} [52], *Pdx1-Cre/Kras*^{G12D}*/p53*$^{-/-}$ [53], *Pdx1-Cre/Kras*^{G12D}*/Smad4*$^{-/-}$ [54], and *Pdx1-Cre/Kras*^{G12D}*/Rb*$^{-/-}$ [55]. AGR2 was abundant in all mPanIN-like stages, including mPanIN-1A, and in the cancer cells in PDAC (Fig. S7). MUC1 was also elevated in mPanIN-like lesions and PDAC, in agreement with previous reports [15, 56], and co-localized with AGR2 (Fig. 5A). Alcian blue, a stain for mucopolysaccharides, also correlated with the sites of AGR2 expression (Fig. 5B). Moreover, AGR2 and MUC1 co-localized in serial sections of human PanIN lesions (Fig. 5C). AGR2 also correlated occasionally with MUC5AC, but poorly with MUC4 (Fig. S8).

Generation of Pdx1-Cre/LSL-Kras^{G12D}/Smad4$^{-/-}$ mice with heterozygous Agr2

Due to the striking *in vitro* data showing that AGR2 expression was both necessary and required for MUC1 expression (Fig. 4), we sought to determine if AGR2 was essential for MUC1 expression *in vivo*. Accordingly, the *Agr2* knockout model [25] was crossed into *Pdx1-Cre/LSL-Kras^{G12D}/Smad4$^{lox/lox}$* mice [54]. This model progresses from mPanIN-like lesions through adenocarcinoma by five months of age, and also develops mucinous cysts [54]. Control mice (*Pdx1-Cre*, *LSL-Kras^{G12D}*, *Smad4$^{lox/lox}$*, or *Agr2$^{-/-}$*) exhibited normal pancreata out to nine months of age. However, as previously shown, *Agr2$^{-/-}$* animals exhibited a high frequency of rectal prolapse and were often moribund by five months [25].

The effects of *Agr2* deficiency were examined in *Pdx1-Cre/LSL-Kras^{G12D}/Smad4$^{lox/lox}$* (P/K/S$^{L/L}$) animals for up to five months. Our final cohort consisted of 14 P/K/S$^{L/L}$, 15 P/K/S$^{L/L}$ with one copy of *Agr2* (P/K/S$^{L/L}$/A$^{+/-}$), and 3 P/K/S$^{L/L}$ with no copies of *Agr2* (P/K/S$^{L/L}$/A$^{-/-}$). Only P/K/S$^{L/L}$, and not P/K/S$^{L/L}$/A$^{+/-}$ or P/K/S$^{L/L}$/A$^{-/-}$, exhibited visible tumor invasion outside the pancreas. Next, histopathological evaluation was performed on sections stained with hematoxylin & eosin (H&E) or Alcian blue and immunostained for CK19 and amylase (Table 1). Sections were evaluated for the presence of acinar-to-ductal metaplasia (ADM), mPanIN1-3, PDAC, and pancreatic cysts by a pancreatic cancer pathologist (DS Longnecker) blinded to the genotype of the pancreatic sections. As previously reported for the P/K/S$^{L/L}$ model [54], by five months of age the pancreata exhibited a high incidence of intraductal papillary mucinous neoplasm (IPMN)-like cysts (5/14), ADM (7/14), mPanIN-like lesions (10/14), and a high proportion (6/14) of "established" PDAC, defined as lesions that contained poorly differentiated, invasive CK19-positive cancer cells. There was also a single "early" PDAC, defined as a small lesion with finger-like loci of CK19-positive cells that were abnormal in appearance and that were in the proximity to advanced PanIN. Many of the established PDAC in these animals were large and, when measurable, averaged five mm at the widest cross-section. Of 14 P/K/S$^{L/L}$ animals, only 2 were histologically normal. By contrast, age-matched P/K/S$^{L/L}$ animals that had only one copy of *Agr2* (P/K/S$^{L/L}$/A$^{+/-}$) developed a much lower incidence of IPMN-like cysts (1/15), ADM (4/15), and mPanIN-like lesions (6/15), and the PDAC was more often an early lesion (5/15), rather than established PDAC (1/15). Only one animal had a measurable tumor (three mm). Of the 15 total P/K/S$^{L/L}$/A$^{+/-}$ animals, almost half (6/15) were histologically normal. Moreover, of three P/K/S$^{L/L}$/A$^{-/-}$ animals, only one developed a single focus of ADM with a small focus of early PDAC.

AGR2 is required for MUC1 expression in pancreatic lesions

We next sought to determine if AGR2 and MUC1 expression was correlated in lesions formed in P/K/S$^{L/+}$ and P/K/S$^{L/L}$ animals that were heterozygous or null for *Agr2*. We used co-IF to stain the sections for AGR2/MUC1 or CK19/amylase, and stained adjacent serial sections using Alcian blue and H&E. Consistent with our study of other mouse models (Figs. 5 and S7), lesions from animals with both alleles of *Agr2* all expressed equivalently high levels of AGR2 and MUC1, and exhibited strong Alcian blue staining (Fig. 6A).

As expected, lesions that developed in P/K/S$^{L/+}$ or P/K/S$^{L/L}$ animals null for *Agr2* lacked expression of AGR2. These lesions were also negative for MUC1 expression and Alcian

blue staining (Fig. 6B). The lesions in P/K/$S^{L/+}$ or P/K/$S^{L/L}$ animals heterozygous for *Agr2* either exhibited uniform AGR2 overexpression, a uniform lack of AGR2, or varied expression of AGR2, sometimes within the same lesion (Fig. 6C-D). In all cases, we saw parallel changes in MUC1 expression and Alcian blue staining (Fig. 6C-D).

Discussion

AGR2 is a potential member of the PDI family of ER-associated enzymes that are endowed with chaperone activity and that catalyze the formation and breakage of disulfide bonds between cysteine residues of proteins, allowing for their proper folding and stable conformation [24-26]. AGR2 was previously implicated as a chaperone to MUC2 in intestinal cells [25], and was recently shown to localize to the ER and to the cell surface of pancreatic cancer cells [38] and to be responsible for ER homeostasis [26]. AGR2 was also promotes the survival, invasion, and metastasis of pancreatic cancer cells, and up-regulates the expression of several ER chaperones, lysosomal proteases cathepsin B and D, and proteins implicated in the ubiquitin-proteosome degradation pathway [38]. Together, these studies underscore the important role of AGR2 in the pathobiology of PDAC.

In the present study we found that AGR2 is abundant in the ER of pancreatic cancer cells, and that its expression is induced with serum starvation. We also determined that AGR2 knockdown enhances endoplasmic reticulum (ER) stress due to the induction of an unfolded protein response (UPR), as evidenced by increased PERK and phospho-PERK levels leading to increased eIF2a phosphorylation in conjunction with increased BiP levels. Inasmuch as UPR-induced ER stress may increase cancer chemosensitivity, these observations suggest that AGR2 downregulation may enhance the responsiveness of pancreatic cancer cells to gemcitabine through this mechanism.

Several lines of evidence indicate that TGF-β-mediated suppression of AGR2 is mediated, at least in part, by SMAD4. First, TGF-β1 reduced AGR2 levels in SMAD4-proficient cells (PANC-1 and COLO-357), but not in BxPC3 cells (homozygous deletion of SMAD4) or in ASPC-1 cells (mutated SMAD4). Second, restoring SMAD4 led to decreased AGR2 mRNA levels. Third, knockdown of SMAD4 in COLO-357 cells increased AGR2 mRNA levels. Fourth, SMAD4 and TGF-β reduced *AGR2* promoter luciferase activity. Inasmuch as a mutation or deletion of SMAD4 disrupts TGF-β signaling in 55% of PDAC [4, 6, 57-60], these findings suggest that loss of SMAD4, by preventing TGF-β-mediated suppression of AGR2, may constitute one mechanism whereby TGF-β converts from a tumor suppressor to a tumor promoter.

Studies using an *Agr2* knockout mouse model indicated that AGR2 is required for mucin production in the intestine and that AGR2 stabilizes MUC2 (a predominant intestinal mucin) via its thioredoxin-like CXXS domain [25]. In the present study we determined that AGR2 and MUC1, but not MUC4 or MUC5AC, co-immunoprecipitated and were tightly co-localized, both in the cytoplasm and in the peri-nuclear space, suggesting that AGR2 and MUC1 might physically interact. Using COLO-357 clones that expressed an inducible AGR2 silencing construct, we determined that suppression of AGR2 expression was associated with a progressive decrease in MUC1 protein, but not RNA levels. Moreover,

engineered expression of mouse AGR2 that was not targeted by the AGR2 silencing construct restored MUC1 protein levels, thereby confirming the tight dependence of MUC1 expression on AGR2 levels. Conversely, the overexpression of AGR2 resulted in increased MUC1 protein levels. Together, these observations suggest that AGR2 increases MUC1 levels in PDAC by preventing MUC1 degradation. Alternatively, as proposed with respect to the actions of AGR2 on MUC2 [25], AGR2 may upregulate MUC1 protein by enhancing MUC1 mRNA translation.

Examining pancreatic cancers arising in four different GEMMs, we determined that AGR2 expression highly overlapped with MUC1 in pancreatic lesions. This co-localization was relatively specific with respect to other MUC proteins, given that AGR2 did not co-localize with either MUC5AC or MUC4, and was also evident in human pancreatic lesions. However, AGR2 was abundant in all mPanIN-like stages in all four tested GEMMs. While its abundance in the *Pdx1-Cre/Kras*^{G12D}*/Smad4*$^{-/-}$ mice supports our findings that AGR2 expression is SMAD4-dependent, other mechanisms must also be in play to lead to its up-regulation in such diverse GEMMs. For example, it is possible that functional perturbations in TGF-β signaling lead to AGR2 up-regulation. Moreover, AGR2 expression has been shown to be increased by FOXA1, FOXA2 [61], the aryl hydrocarbon receptor [62], estrogen [63] and androgens [64], and to be downregulated by ErbB3 binding protein 1 [61]. It is likely, therefore, that there are numerous mechanisms that regulate AGR2 expression in the SMAD4-intact pancreas.

To determine whether elevated MUC1 levels could be seen in lesions devoid of AGR2 expression, we bred *Agr2* knockout mice [25] into a GEMM where *Smad4* deletion and *Kras*^{G12D} activation is confined to the pancreas using the pancreas-specific promoter, Pdx1 [54]. Since homozygous *Agr2* knockouts develop extra-pancreatic complications (e.g., rectal prolapse [25]), we focused our studies on *Agr2* heterozygotes. Accordingly, we bred animals with homozygous loss of *Smad4* (P/K/S$^{L/L}$) and either wild type or heterozygous expression of *Agr2* and collected pancreata at regular intervals. mPanIN-like or cancer lesions that either lacked or had varied expression of AGR2 exhibited parallel changes in MUC1 expression. AGR2 entirely co-localized with MUC1 and Alcian blue. Thus, the *in vivo* data corroborate our conclusions based on the *in vitro* results that AGR2 is necessary and sufficient for MUC1 expression.

We next examined the tumor incidence of age-matched animals in our cohort. Strikingly, P/K/S$^{L/L}$/A$^{+/-}$ animals had significantly fewer pancreatic lesions than their wild type *Agr2* counterparts (P/K/S$^{L/L}$; Table 1). Thus, 40% (6/15) of the P/K/S$^{L/L}$/A$^{+/-}$ animals were histologically normal with no detectable pancreatic lesions, compared to only 14% (2/14) of age-matched P/K/S$^{L/L}$ controls. This is the first study using a GEMM of PDAC to address the role of AGR2 in PDAC initiation and progression. Strikingly, mice deficient in even one allele of *Agr2* exhibited a delay in PDAC initiation, or altogether failed to progress to PDAC. These observations suggest that AGR2 is a crucial component of a pathway that leads to malignant transformation downstream of oncogenic K-ras.

The mechanisms by which AGR2 contributes to PDAC initiation are not readily evident. Nonetheless, it is well established that MUC1 is directly implicated in PDAC progression,

through its effects on cell-to-cell signaling [19], induction of EMT [65], EGFR activation [20, 21], and HER2 signaling [22]. Deletion of *Muc1* in a tumor model of pancreatic cancer slowed tumor progression and resulted in a lower rate of metastasis [66]. Therefore, our observation that AGR2 is required for high levels of MUC1 protein raise the possibility that AGR2 interacts with MUC1 to promote PanIN formation and progression to PDAC. Taken together, our study delineates a previously unknown link between TGF-β and MUC1, through the candidate oncogene AGR2, and suggests that AGR2 is crucial for PanIN initiation and PDAC progression (Fig. 7). These observations raise the possibility that AGR2 is a novel molecular target for both the prevention and treatment of PDAC.

Methods

Cell Culture and Treatments

ASPC-1 (ATCC CRL-1682), BxPC3 (ATCC CRL-1687), PANC-1 (ATCC CRL-1469), and COLO-357 (a gift from R.S. Metzgar, Duke University) human pancreatic cells were maintained using either DMEM/F12 (COLO-357 and PANC-1) or RPMI (ASPC-1 and T3M4) media containing 10% fetal bovine serum (FBS) from Omega Scientific Inc. (Tarzana, CA), 100 U/mL penicillin, and 100 μg/mL streptomycin.

For experiments with TGF-β1, cells were incubated for 24 hours in serum-free medium with 500 pM TGF-β1 as previously reported [67]. For experiments with doxycycline (DOX), cells were grown in media containing tetracycline-free FBS and 1-2 μM DOX. Stably infected *pTRIPZ-AGR2* single-cell clones were selected using 1-2 μg/mL puromycin and stably transfected *pcDNA-AGR2* cells were maintained in selective medium containing 400 μg/mL G418. For visualization of the endoplasmic reticulum (ER), live cells were stained with ER Tracker® according to manufacturer protocol (Invitrogen, Carlsbad CA) after transient transfection with *RFP-sham* or *AGR2-RFP*.

Plasmids and Transduction

To generate the *AGR2-luc* reporter plasmid, a 2598 bp fragment of the *AGR2* 5′UTR was PCR amplified (forward: 5′-GGACCCATAGACACTGTGGACC-3′; reverse: 5′-CGGTCCAAGCTTCTGAGTG-3′) from human genomic DNA (Promega, Madison, WI), cloned into the pGL3 vector (Promega, Madison, WI), and verified by sequencing. Plasmids were obtained from: *SBE4-Luc* TGF-β reporter (Addgene #16495; [50]), *pCMV5-DPC-HA* SMAD4 (Addgene #14038; [49]), two *pTRIPZ-AGR2* plasmids (Open Biosystems, Huntsville, AL; V2THS_251763, V2THS_199455), *pcDNA-AGR2* and *AGR2-RFP* (Ted R. Hupp; University of Edinburgh). Transfections were performed using Lipofectamine 2000 (Invitrogen, Carlsbad CA) according to manufacturer recommendations or transduced by lentiviral infection.

RNA Isolation & Taqman Analysis

RNA extracts were prepared using the Qiagen RNeasy Mini Kit and the on-column RNase-free DNase set (Qiagen, Germantown MD). cDNA was synthesized using the Superscript III First-Strand Synthesis System (Invitrogen, Carlsbad, CA). Quantitative PCR was performed using the Taqman gene expression primer/probe TAMRA sets and an ABI PRISM 7700

Sequence Detection System (Applied Biosystems, Foster City, CA). All Ct data were normalized to the 18S VIC-internal control and delta Ct values were calculated.

Immunoblotting

Cell lysates were prepared and electrophoresed as previously reported [55]. The following antibodies were used for immunoblotting: polyclonal anti-AGR2 antibody (Imgenex, San Diego, CA; 1:250), monoclonal anti-AGR2 antibody (Imgenex, San Diego, CA; 1:500). monoclonal anti-MUC1 antibody (MA552MUC1-CORE; Novocastra, Buffalo Grove, IL; 1:200), monoclonal anti-MUC5AC antibody (CLH2 MUC-5AC-CE; Novocastra, Buffalo Grove IL; 1:100), monoclonal anti-MUC4 antibody (ab60720, Abcam, Cambridge MA; 1:500), anti-phosphorylated or total eIF2α antibody (Cell Signaling, Danvers, MA; 1:1000), anti-phosphorylated or total PERK antibody (Cell Signaling, Danvers, MA; 1:1000), anti-GRP78 antibody (Santa Cruz Biotechnology, Santa Cruz, CA; 1:200) or an anti-ERK2 antibody (Santa Cruz Biotechnology, Santa Cruz, CA; 1:7000).

Luciferase Assay

Reporter constructs (*SBE4-Luc*; *AGR2-Luc*) were co-transfected with *CMV-Renilla* using Lipofectamine 2000 (Invitrogen, Carlsbad, CA). Luciferase activity was determined using the Dual Luciferase Assay kit (Promega, Madison, WI) and an LMaxII microplate reader (Molecular Devices, Sunnyvale, CA). All assays were performed in triplicate, measured in duplicate, and normalized to internal controls.

Immunohistochemistry (IHC)/Immunofluorescence (IF)

Fixation, embedding, antigen retrieval, and IHC were all performed as previously reported [55]. For multiplexed IF, primary antibodies were co-incubated and incubated with fluorescently conjugated secondary antibodies (Molecular Probes, Carlsbad, CA). Alcian blue staining was performed as described [68].

For co-localization studies in cells, human pancreatic cells were plated in 8-well chambers on a glass slide. Cells were fixed using formalin, permeabilized using 0.05% Triton-X, and blocked with 5% BSA/1% goat serum. Cells were co-incubated with the appropriate antibodies for one hour at room temperature and then with fluorescently conjugated secondary antibodies.

Immunoprecipitation (IP)

An IP was performed using 500 μg of protein from PANC-1 cells, polyclonal anti-AGR2 antibody (Imgenex, San Diego CA), and protein A/G agarose beads, according to manufacturer protocol (Santa Cruz Biotechnologies, Santa Cruz CA). Denatured supernatant from the pull-downs was immunoblotted for mucins, as described above. For negative controls, an IgG antibody or A/G beads, alone, were used in the IP. AGR2 was immunoblotted in each experiment as a positive control..

Image Capture and Analysis

All images were taken using an Olympus BX60 microscope equipped with an Olympus DP70 camera and ImagePro software. For fluorescent images, individual monochrome pictures were captured for each channel and then merged using Adobe Photoshop CS3 software (version 10.0.1). Live cells were imaged using the Confocal Microscopy Core at Dartmouth Medical School.

Mouse husbandry

Breeding was initiated with: *LSL-Kras*^{G12D} mice (01×J6-B6.129-*Kras2*^{tm4Tyj}, Mouse Models of Human Cancers Consortium, National Cancer Institute, Frederick, MD, [52]). *Pdx1-Cre* mice (G. Gu [69]), Smad4$^{lox/lox}$ mice (N. Bardeesy [54]), and *Agr2*$^{-/-}$ mice (D. Erle [25]). Founder strains were bred to generate *Pdx1-Cre/LSL-Kras*^{G12D}*/Smad4*$^{lox/lox}$ as previously described [54] with or without loss of *Agr2*. All studies with mice were approved by the Dartmouth Medical School and Indiana University School of Medicine Institutional Animal Care and Use Committees.

Supplementary Material

Refer to Web version on PubMed Central for supplementary material.

Acknowledgements

We thank Dr. Ted R. Hupp (U. of Edinburgh) for the *AGR2-RFP* and *pcDNA-AGR2* plasmids; Dr. Park (UCSF) for providing the *Agr2*$^{-/-}$ mice; Dr. J. Gore for helpful discussions; and Ms. Catherine Chen for excellent laboratory work. This research was supported by the U.S. Public Health Service Grant CA-R37-075059, awarded by the National Cancer Institute to M.K. A.M.N. was supported by the NRSA Molecular and Toxicology Program fellowship 5T32CA009658-18. A. Balboni was supported by the Program in Experimental and Molecular Medicine.

References

1. Cancer Facts & Figures 2007. American Cancer Society; Atlanta: 2007.
2. Norris, AM.; Korc, M. Smad4/TGF-b pathway: signaling pathways in pancreatic pathogenesis. In: Neoptolemos, JP.; Buchler, M.; Errutia, R., editors. Pancreatic Cancer. Springer; New York: 2009.
3. Hruban RH, Wilentz RE, Kern SE. Genetic Progression in the Pancreatic Ducts. Am J Pathol. 2000; 156(6):1821–1825. [PubMed: 10854204]
4. van Heek T, Rader AE, Offerhaus GJ, McCarthy DM, Goggins M, Hruban RH, et al. K-ras, p53, and DPC4 (MAD4) alterations in fine-needle aspirates of the pancreas: a molecular panel correlates with and supplements cytologic diagnosis. Am J Clin Pathol. 2002; 117(5):755–65. [PubMed: 12090425]
5. Hansel DE, Kern SE, Hruban RH. Molecular pathogenesis of pancreatic cancer. Annu Rev Genomics Hum Genet. 2003; 4:237–56. [PubMed: 14527303]
6. Hahn SA, Schutte M, Hoque AT, Moskaluk CA, da Costa LT, Rozenblum E, et al. DPC4, a candidate tumor suppressor gene at human chromosome 18q21.1. Science. 1996; 271(5247):350–3. [PubMed: 8553070]
7. Wagner M, Kleeff J, Lopez ME, Bockman I, Massaque J, Korc M. Transfection of the type I TGF-beta receptor restores TGF-beta responsiveness in pancreatic cancer. Int J Cancer. 1998; 78(2):255–60. [PubMed: 9754660]
8. Baldwin RL, Friess H, Yokoyama M, Lopez ME, Kobrin MS, Buchler MW, et al. Attenuated ALK5 receptor expression in human pancreatic cancer: correlation with resistance to growth inhibition. Int J Cancer. 1996; 67(2):283–8. [PubMed: 8760600]

9. Kleeff J, Maruyama H, Friess H, Buchler MW, Falb D, Korc M. Smad6 suppresses TGF-beta-induced growth inhibition in COLO-357 pancreatic cancer cells and is overexpressed in pancreatic cancer. Biochem Biophys Res Commun. 1999; 255(2):268–73. [PubMed: 10049697]

10. Arnold NB, Ketterer K, Kleeff J, Friess H, Buchler MW, Korc M. Thioredoxin is downstream of Smad7 in a pathway that promotes growth and suppresses cisplatin-induced apoptosis in pancreatic cancer. Cancer Res. 2004; 64(10):3599–606. [PubMed: 15150118]

11. Friess H, Yamanaka Y, Buchler M, Ebert M, Beger HG, Gold LI, et al. Enhanced expression of transforming growth factor beta isoforms in pancreatic cancer correlates with decreased survival. Gastroenterology. 1993; 105(6):1846–56. [PubMed: 8253361]

12. Sempere LF, Gunn JR, Korc M. A novel 3-dimensional culture system uncovers growth stimulatory actions by TGFbeta in pancreatic cancer cells. Cancer Biol Ther. 2011; 12(3):198–207. [PubMed: 21613822]

13. Kufe DW. Mucins in cancer: function, prognosis and therapy. Nat Rev Cancer. 2009; 9(12):874–85. [PubMed: 19935676]

14. Moniaux N, Andrianifahanana M, Brand RE, Batra SK. Multiple roles of mucins in pancreatic cancer, a lethal and challenging malignancy. Br J Cancer. 2004; 91(9):1633–8. [PubMed: 15494719]

15. Levi E, Klimstra DS, Andea A, Basturk O, Adsay NV. MUC1 and MUC2 in pancreatic neoplasia. J Clin Pathol. 2004; 57(5):456–62. [PubMed: 15113850]

16. Balague C, Gambus G, Carrato C, Porchet N, Aubert JP, Kim YS, et al. Altered expression of MUC2, MUC4, and MUC5 mucin genes in pancreas tissues and cancer cell lines. Gastroenterology. 1994; 106(4):1054–61. [PubMed: 8143972]

17. Choudhury A, Moniaux N, Winpenny JP, Hollingsworth MA, Aubert JP, Batra SK. Human MUC4 mucin cDNA and its variants in pancreatic carcinoma. J Biochem. 2000; 128(2):233–43. [PubMed: 10920259]

18. Andrianifahanana M, Moniaux N, Schmied BM, Ringel J, Friess H, Hollingsworth MA, et al. Mucin (MUC) gene expression in human pancreatic adenocarcinoma and chronic pancreatitis: a potential role of MUC4 as a tumor marker of diagnostic significance. Clin Cancer Res. 2001; 7(12):4033–40. [PubMed: 11751498]

19. Yamamoto M, Bharti A, Li Y, Kufe D. Interaction of the DF3/MUC1 breast carcinoma-associated antigen and beta-catenin in cell adhesion. J Biol Chem. 1997; 272(19):12492–4. [PubMed: 9139698]

20. Li Y, Ren J, Yu W, Li Q, Kuwahara H, Yin L, et al. The epidermal growth factor receptor regulates interaction of the human DF3/MUC1 carcinoma antigen with c-Src and beta-catenin. J Biol Chem. 2001; 276(38):35239–42. [PubMed: 11483589]

21. Schroeder JA, Thompson MC, Gardner MM, Gendler SJ. Transgenic MUC1 interacts with epidermal growth factor receptor and correlates with mitogen-activated protein kinase activation in the mouse mammary gland. J Biol Chem. 2001; 276(16):13057–64. [PubMed: 11278868]

22. Carraway KL, Perez A, Idris N, Jepson S, Arango M, Komatsu M, et al. Muc4/sialomucin complex, the intramembrane ErbB2 ligand, in cancer and epithelia: to protect and to survive. Prog Nucleic Acid Res Mol Biol. 2002; 71:149–85. [PubMed: 12102554]

23. Pohler E, Craig AL, Cotton J, Lawrie L, Dillon JF, Ross P, et al. The Barrett's antigen anterior gradient-2 silences the p53 transcriptional response to DNA damage. Mol Cell Proteomics. 2004; 3(6):534–47. [PubMed: 14967811]

24. Persson S, Rosenquist M, Knoblach B, Khosravi-Far R, Sommarin M, Michalak M. Diversity of the protein disulfide isomerase family: identification of breast tumor induced Hag2 and Hag3 as novel members of the protein family. Mol Phylogenet Evol. 2005; 36(3):734–40. [PubMed: 15935701]

25. Park SW, Zhen G, Verhaeghe C, Nakagami Y, Nguyenvu LT, Barczak AJ, et al. The protein disulfide isomerase AGR2 is essential for production of intestinal mucus. Proc Natl Acad Sci U S A. 2009; 106(17):6950–5. [PubMed: 19359471]

26. Higa A, Mulot A, Delom F, Bouchecareilh M, Nguyen DT, Boismenu D, et al. Role of pro-oncogenic protein disulfide isomerase (PDI) family member anterior gradient 2 (AGR2) in the

control of endoplasmic reticulum homeostasis. J Biol Chem. 2011; 286(52):44855–68. [PubMed: 22025610]

27. Liu D, Rudland PS, Sibson DR, Platt-Higgins A, Barraclough R. Human homologue of cement gland protein, a novel metastasis inducer associated with breast carcinomas. Cancer Res. 2005; 65(9):3796–805. [PubMed: 15867376]
28. Fritzsche FR, Dahl E, Pahl S, Burkhardt M, Luo J, Mayordomo E, et al. Prognostic relevance of AGR2 expression in breast cancer. Clin Cancer Res. 2006; 12(6):1728–34. [PubMed: 16551856]
29. Kristiansen G, Pilarsky C, Wissmann C, Kaiser S, Bruemmendorf T, Roepcke S, et al. Expression profiling of microdissected matched prostate cancer samples reveals CD166/MEMD and CD24 as new prognostic markers for patient survival. J Pathol. 2005; 205(3):359–76. [PubMed: 15532095]
30. Hrstka R, Nenutil R, Fourtouna A, Maslon MM, Naughton C, Langdon S, et al. The pro-metastatic protein anterior gradient-2 predicts poor prognosis in tamoxifen-treated breast cancers. Oncogene. 2010; 29(34):4838–47. [PubMed: 20531310]
31. Innes HE, Liu D, Barraclough R, Davies MP, O'Neill PA, Platt-Higgins A, et al. Significance of the metastasis-inducing protein AGR2 for outcome in hormonally treated breast cancer patients. Br J Cancer. 2006; 94(7):1057–65. [PubMed: 16598187]
32. Riener MO, Pilarsky C, Gerhardt J, Grutzmann R, Fritzsche FR, Bahra M, et al. Prognostic significance of AGR2 in pancreatic ductal adenocarcinoma. Histol Histopathol. 2009; 24(9):1121–8. [PubMed: 19609859]
33. Chen R, Pan S, Duan X, Nelson BH, Sahota RA, de Rham S, et al. Elevated level of anterior gradient-2 in pancreatic juice from patients with pre-malignant pancreatic neoplasia. Mol Cancer. 2010; 9:149. [PubMed: 20550709]
34. Brychtova V, Vojtesek B, Hrstka R. Anterior gradient 2: A novel player in tumor cell biology. Cancer Lett. 2011; 304(1):1–7. [PubMed: 21371820]
35. Thompson DA, Weigel RJ. hAG-2, the human homologue of the Xenopus laevis cement gland gene XAG-2, is coexpressed with estrogen receptor in breast cancer cell lines. Biochem Biophys Res Commun. 1998; 251(1):111–6. [PubMed: 9790916]
36. Lowe AW, Olsen M, Hao Y, Lee SP, Taek Lee K, Chen X, et al. Gene expression patterns in pancreatic tumors, cells and tissues. PLoS ONE. 2007; 2(3):e323. [PubMed: 17389914]
37. Iacobuzio-Donahue CA, Maitra A, Olsen M, Lowe AW, van Heek NT, Rosty C, et al. Exploration of global gene expression patterns in pancreatic adenocarcinoma using cDNA microarrays. Am J Pathol. 2003; 162(4):1151–62. [PubMed: 12651607]
38. Dumartin L, Whiteman HJ, Weeks ME, Hariharan D, Dmitrovic B, Iacobuzio-Donahue CA, et al. AGR2 is a novel surface antigen that promotes the dissemination of pancreatic cancer cells through regulation of cathepsins B and D. Cancer Res. 2011; 71(22):7091–102. [PubMed: 21948970]
39. Wang Z, Hao Y, Lowe AW. The adenocarcinoma-associated antigen, AGR2, promotes tumor growth, cell migration, and cellular transformation. Cancer Res. 2008; 68(2):492–7. [PubMed: 18199544]
40. Ramachandran V, Arumugam T, Wang H, Logsdon CD. Anterior gradient 2 is expressed and secreted during the development of pancreatic cancer and promotes cancer cell survival. Cancer Res. 2008; 68(19):7811–8. [PubMed: 18829536]
41. Chang KC, Komm B, Arnold NB, Korc M. The application of differential display as a gene profiling tool. Methods Mol Biol. 2007; 383:31–40. [PubMed: 18217677]
42. Hahn SA, Hoque AT, Moskaluk CA, da Costa LT, Schutte M, Rozenblum E, et al. Homozygous deletion map at 18q21.1 in pancreatic cancer. Cancer Res. 1996; 56(3):490–4. [PubMed: 8564959]
43. Sipos B, Moser S, Kalthoff H, Torok V, Lohr M, Kloppel G. A comprehensive characterization of pancreatic ductal carcinoma cell lines: towards the establishment of an in vitro research platform. Virchows Arch. 2003; 442(5):444–52. [PubMed: 12692724]
44. Heldin CH, Miyazono K, ten Dijke P. TGF-beta signalling from cell membrane to nucleus through SMAD proteins. Nature. 1997; 390(6659):465–71. [PubMed: 9393997]
45. Dennler S, Itoh S, Vivien D, ten Dijke P, Huet S, Gauthier J-M. Direct binding of Smad3 and Smad4 to critical TGF[beta]-inducible elements in the promoter of human plasminogen activator inhibitor-type 1 gene. EMBO J. 1998; 17(11):3091–3100. [PubMed: 9606191]

46. Massague J, Seoane J, Wotton D. Smad transcription factors. Genes Dev. 2005; 19(23):2783–810. [PubMed: 16322555]
47. Jonk LJC, Itoh S, Heldin C-H, ten Dijke P, Kruijer W. Identification and Functional Characterization of a Smad Binding Element (SBE) in the JunB Promoter That Acts as a Transforming Growth Factor-OE≤, Activin, and Bone Morphogenetic Protein-inducible Enhancer. Journal of Biological Chemistry. 1998; 273(33):21145–21152. [PubMed: 9694870]
48. Zheng W, Rosenstiel P, Huse K, Sina C, Valentonyte R, Mah N, et al. Evaluation of AGR2 and AGR3 as candidate genes for inflammatory bowel disease. Genes Immun. 2006; 7(1):11–8. [PubMed: 16222343]
49. Lagna G, Hata A, Hemmati-Brivanlou A, Massague J. Partnership between DPC4 and SMAD proteins in TGF-beta signalling pathways. Nature. 1996; 383(6603):832–6. [PubMed: 8893010]
50. Zawel L, Dai JL, Buckhaults P, Zhou S, Kinzler KW, Vogelstein B, et al. Human Smad3 and Smad4 are sequence-specific transcription activators. Mol Cell. 1998; 1(4):611–7. [PubMed: 9660945]
51. Forstner G. Signal transduction, packaging and secretion of mucins. Annu Rev Physiol. 1995; 57:585–605. [PubMed: 7778879]
52. Hingorani SR, Petricoin EF, Maitra A, Rajapakse V, King C, Jacobetz MA, et al. Preinvasive and invasive ductal pancreatic cancer and its early detection in the mouse. Cancer Cell. 2003; 4(6): 437–50. [PubMed: 14706336]
53. Bardeesy N, Aguirre AJ, Chu GC, Cheng KH, Lopez LV, Hezel AF, et al. Both p16(Ink4a) and the p19(Arf)-p53 pathway constrain progression of pancreatic adenocarcinoma in the mouse. Proc Natl Acad Sci U S A. 2006; 103(15):5947–52. [PubMed: 16585505]
54. Bardeesy N, Cheng KH, Berger JH, Chu GC, Pahler J, Olson P, et al. Smad4 is dispensable for normal pancreas development yet critical in progression and tumor biology of pancreas cancer. Genes Dev. 2006; 20(22):3130–46. [PubMed: 17114584]
55. Carriere C, Gore AJ, Norris AM, Gunn JR, Young AL, Longnecker DS, et al. Deletion of rb accelerates pancreatic carcinogenesis by oncogenic kras and impairs senescence in premalignant lesions. Gastroenterology. 2011; 141(3):1091–101. [PubMed: 21699781]
56. Nagata K, Horinouchi M, Saitou M, Higashi M, Nomoto M, Goto M, et al. Mucin expression profile in pancreatic cancer and the precursor lesions. J Hepatobiliary Pancreat Surg. 2007; 14(3): 243–54. [PubMed: 17520199]
57. Riggins GJ, Thiagalingam S, Rozenblum E, Weinstein CL, Kern SE, Hamilton SR, et al. Mad-related genes in the human. Nat Genet. 1996; 13(3):347–9. [PubMed: 8673135]
58. Jaffee EM, Hruban RH, Canto M, Kern SE. Focus on pancreas cancer. Cancer Cell. 2002; 2(1):25–8. [PubMed: 12150822]
59. Wilentz RE, Iacobuzio-Donahue CA, Argani P, McCarthy DM, Parsons JL, Yeo CJ, et al. Loss of expression of Dpc4 in pancreatic intraepithelial neoplasia: evidence that DPC4 inactivation occurs late in neoplastic progression. Cancer Res. 2000; 60(7):2002–6. [PubMed: 10766191]
60. Wilentz RE, Hruban RH. Pathology of cancer of the pancreas. Surg Oncol Clin N Am. 1998; 7(1): 43–65. [PubMed: 9443986]
61. Zhang X, Ali TZ, Hua Z. ErbB3 Binding Protein 1 Represses Metastasis-Promoting Gene Anterior Gradient Protein 2 in Prostate Cancer. Cancer Res. 2010; 70:240–248. [PubMed: 20048076]
62. Ambolet-Camoit A, Bui LC, Pierre S, Chevallier A, Marchand A, Coumoul X, et al. 2,3,7,8-Tetrachlorodibenzo-*p*-Dioxin Counteracts the p53 Response to a Genotoxicant by Upregulating Expression of the Metastasis Marker AGR2 in the Hepatocarcinoma Cell Line HepG2. Toxicological Sciences. 2010; 115(2):501–512. [PubMed: 20299546]
63. Wilson CL, Sims AH, Howell A, Miller CJ, Clarke RB. Effects of oestrogen on gene expression in epithelium and stroma of normal human breast tissue. Endocrine-Related Cancer. 2006; 13(2): 617–628. [PubMed: 16728587]
64. Zhang JS, Gong A, Cheville JC, Smith DI, Young CY. AGR2, an androgen-inducible secretory protein overexpressed in prostate cancer. Genes Chromosomes Cancer. 2005; 43(3):249–59. [PubMed: 15834940]

65. Roy LD, Sahraei M, Subramani DB, Besmer D, Nath S, Tinder TL, et al. MUC1 enhances invasiveness of pancreatic cancer cells by inducing epithelial to mesenchymal transition. Oncogene. 2011; 30(12):1449–59. [PubMed: 21102519]

66. Besmer DM, Curry JM, Roy LD, Tinder TL, Sahraei M, Schettini J, et al. Pancreatic ductal adenocarcinoma mice lacking mucin 1 have a profound defect in tumor growth and metastasis. Cancer Res. 2011; 71(13):4432–42. [PubMed: 21558393]

67. Boyer Arnold N, Korc M. Smad7 abrogates transforming growth factor-beta1-mediated growth inhibition in COLO-357 cells through functional inactivation of the retinoblastoma protein. J Biol Chem. 2005; 280(23):21858–66. [PubMed: 15811853]

68. Carriere C, Seeley ES, Goetze T, Longnecker DS, Korc M. The Nestin progenitor lineage is the compartment of origin for pancreatic intraepithelial neoplasia. Proc Natl Acad Sci U S A. 2007; 104(11):4437–42. [PubMed: 17360542]

69. Gu G, Dubauskaite J, Melton DA. Direct evidence for the pancreatic lineage: NGN3+ cells are islet progenitors and are distinct from duct progenitors. Development. 2002; 129(10):2447–57. [PubMed: 11973276]

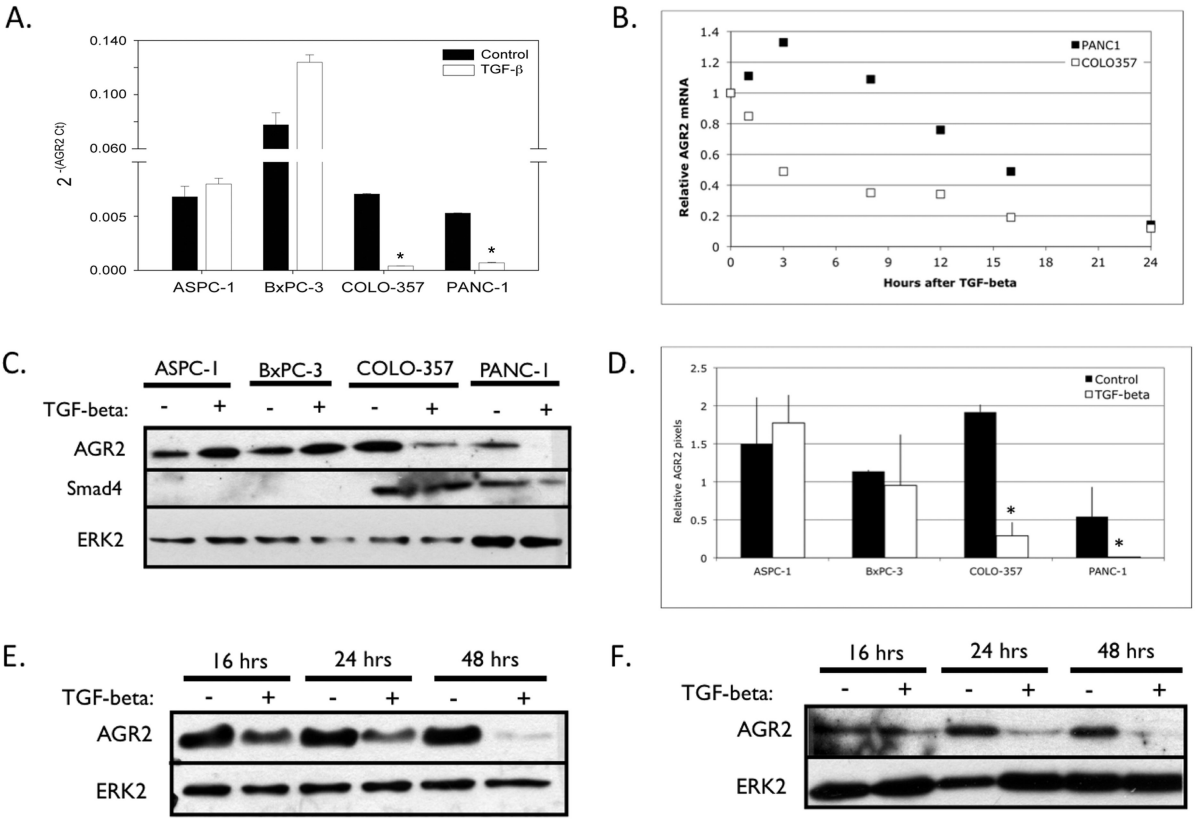

Figure 1. AGR2 is a downstream target of TGF-β signaling

(A) Quantitative RT-PCR of AGR2 mRNA, 24 hrs after addition of 500 pM TGF-β1, in ASPC-1, BxPC3, COLO-357, and PANC-1 cells. Data are the means ± SEM from at least three experiments. *$p < 0.01$, compared with respective controls. **(B)** The levels of AGR2 RNA were determined by quantitative RT-PCR following addition of 500 pM TGF-β1 for 0, 1, 3, 8, 12, 16, and 24 hrs in COLO-357 (white) and PANC-1 (black). The points plotted are the average of two experiments at each time point. **(C)** Western blot of AGR2, SMAD4, and ERK2 (loading control) in ASPC-1, BxPC3, COLO-357, and PANC-1 cells after 48 hrs of incubation with 500 pM TGF-β1. T3M4 cells had no detectable levels of AGR2 protein. **(D)** Densitometry of AGR2 immunoreactivity following 48 hrs of TGF-β in ASPC-1, BxPC3, COLO-357, and PANC-1. The mean pixel density of AGR2 was quantitated and normalized to its corresponding ERK2 (loading control). Data are the means ± SEM from at least three experiments.*$p < 0.01$, compared to untreated control. **(E)** Western blot of AGR2 and ERK2 (loading control) in PANC-1 cells after 16, 24, and 48 hrs incubation with TGF-β1. **(F)** Western blot of AGR2 and ERK2 (loading control) in COLO-357 after 16, 24, and 48 hrs incubation with 500 pM TGF-β1.

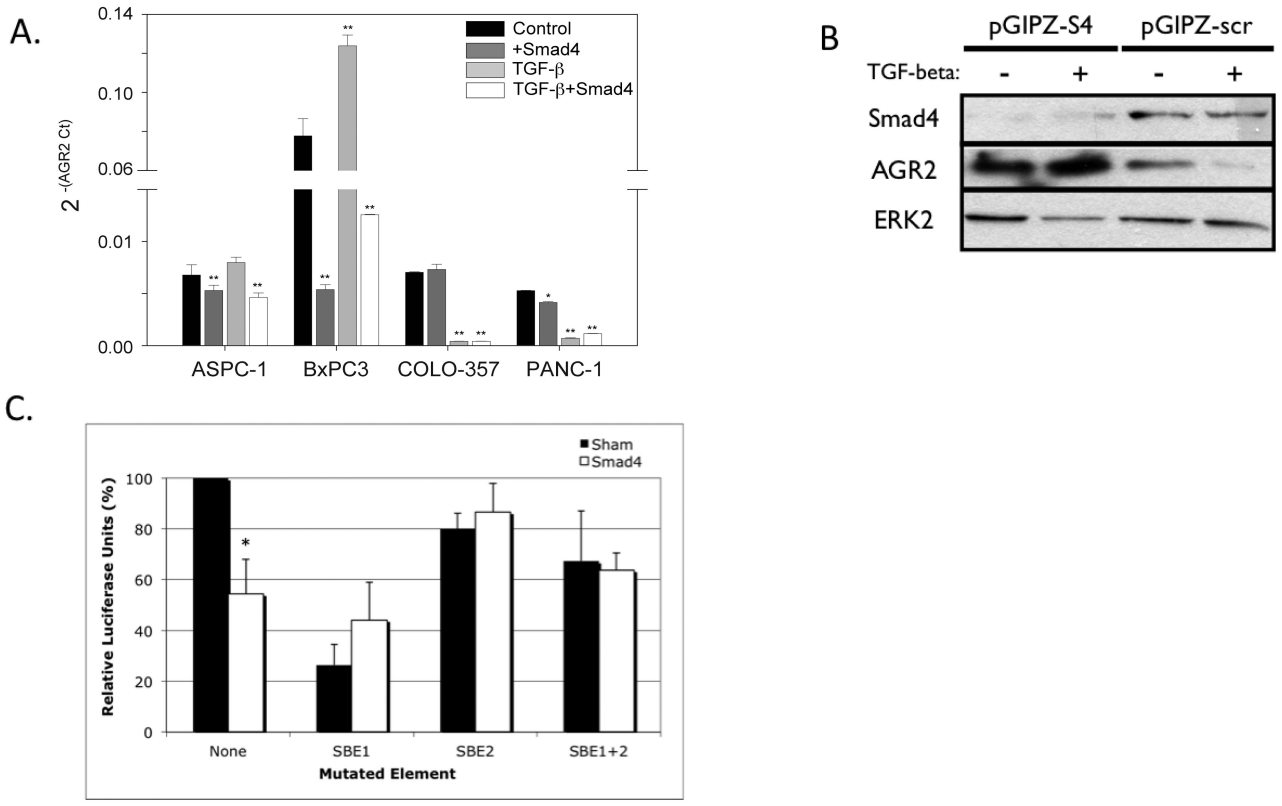

Figure 2. AGR2 is a transcriptional target of SMAD4

(A) Quantitative RT-PCR of AGR2 RNA levels in ASPC-1, BxPC3, COLO-357, and PANC-1 cells with CMV-HA sham alone, CMV-SMAD4, CMV-HA sham/TGF-β, or CMV-SMAD4/TGF-β. Data are the means ± SEM from at least three experiments. **p* < 0.05, and ***p* < 0.01 compared to respective controls. **(B)** A western blot showing SMAD4, AGR2, and ERK2 (loading control) protein levels in COLO-357 cells stably expressing either pGIPZ-SMAD4 (left) or pGIPZ-scrambled (right) shRNA silencing vectors, with or without treatment with TGF-β. **(C)** A luciferase assay using the AGR2-luc reporter with either wild-type, mutated SBE1, mutated SBE2, or with both SBEs mutated and with co-transfection of either CMV-HA sham or CMV-SMAD4 in PANC-1. Percent luciferase units relative to wild-type and untreated AGR2-luc control are shown, after normalization to a Renilla internal control for transfection and cell lysis. Data are the means ± SEM from three experiments. **p* < 0.01 compared with respective control.

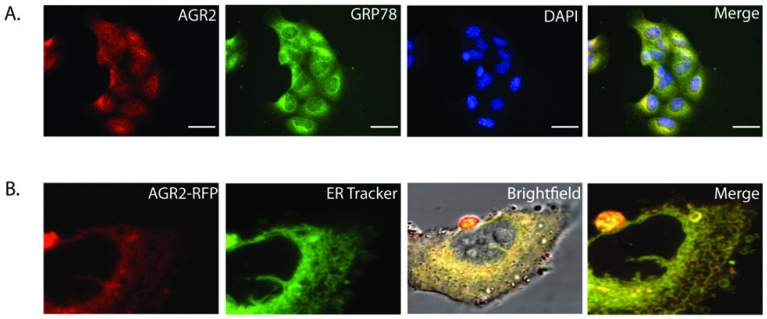

Figure 3. AGR2 localizes to the endoplasmic reticulum of pancreatic cancer cells

(A) Immunofluorescence of AGR2 and an endoplasmic reticulum (ER)-associated protein, GRP78, in PANC-1 cells. AGR2 is shown in red, GRP78 in green, DAPI (nuclear stain) in blue, and the merged image of all three on the far right. Yellow color indicates areas of co-localization of AGR2 and GRP78. Magnification: 400×; Scale bar: 10 μm. **(B)** Live cell confocal imaging of a PANC-1 cell expressing an AGR2-RFP fusion protein (left panel) and stained with an ER-targeted dye (ER Tracker©. The merged AGR-RFP/ER Tracker signal is shown on the far right. The brightfield picture, with merged colors, is also pictured in the middle right for reference.

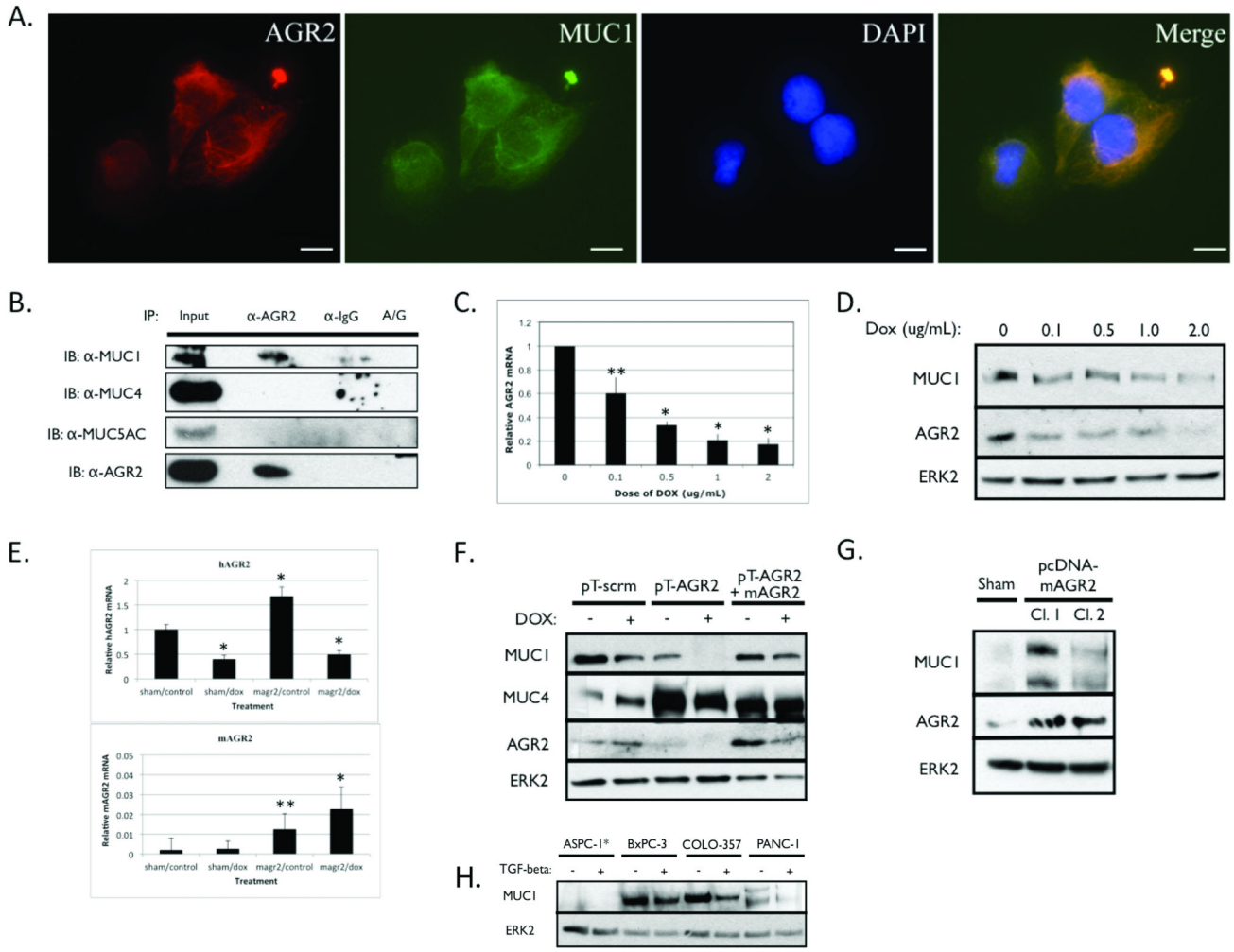

Figure 4. AGR2 interacts with and is required for MUC1 protein expression

(A) Immunofluorescence of AGR2 (red), MUC1 (green), and DAPI (blue) in PANC-1 cells. The merged image is in the far right panel. Yellow color indicates where AGR2 and MUC1 co-localize. Magnification: 800×; Scale bar: five μm. **(B)** Immunoprecipitation using anti-AGR2, mouse IgG, or no antibody (A/G beads only) and blotting for MUC1, MUC4, MUC5AC, or AGR2. Input is 1/10 the total protein used in the precipitation. Lysates shown were prepared from PANC-1. **(C)** Quantitative RT-PCR of AGR2 mRNA in stable COLO-357 cells expressing pTRIPZ-AGR2 (doxycycline-inducible silencing vector) and treated with 0, 0.1, 0.5, 1.0, or 2.0 ug/mL doxycycline for 72 hrs. Data are the means ± SEM of three experiments. **(D)** Western blot for MUC1, AGR2, or ERK2 (loading control) in stable COLO-357-pTRIPZ-AGR2 cells treated with 0, 0.1, 0.5, 1.0, or 2.0 ug/mL doxycycline for 72 hrs. **(E)** Quantitative RT-PCR of human (hAGR2, top) and mouse (mAGR2, bottom) AGR2 in stable COLO-357-pTRIPZ-AGR2 cells transiently transfected either with empty pcDNA vector (sham) or a pcDNA-AGR2 expression vector (magr2) and untreated or treated with 1 ug/mL DOX for 72 hrs. Data are the average ± SD from two experiments. **(F)** Western blot for MUC1, MUC4, AGR2, or ERK2 (loading control) in untreated, DOX-treated stable COLO-357-pTRIPZ-scramble (pT-scrm), or COLO-357-

pTRIPZ-AGR2 cells transiently transfected with either empty pcDNA vector (pT-AGR2) or pcDNA-mAGR2 (pT-AGR2 + AGR2). **(G)** Western blot for MUC1, AGR2, and ERK2 (loading control) in stable PANC-1 clones transfected either with empty pcDNA vector (sham; first lane) or pcDNA-AGR2 (Cl.1 and Cl.2; second and third lanes). MUC1 migrates as a doublet in PANC-1 cells. **(H)** Western blot of MUC1 and ERK2 (loading control) in ASPC-1, BxPC-3, COLO-357, and PANC-1 cells incubated in the absence or presence of 500 pM TGF-β1. *MUC1 was not detectable in ASPC-1 cells and migrated as a doublet in PANC-1 cells.

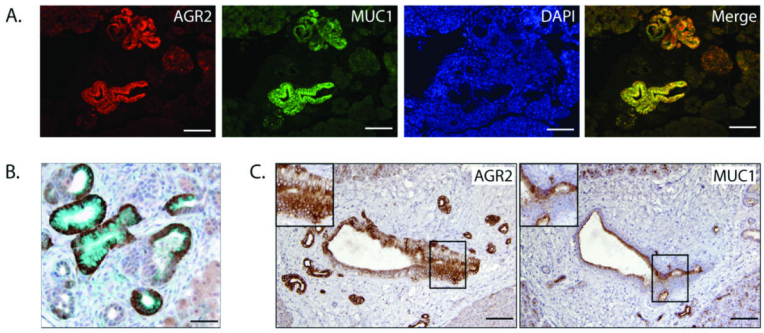

Figure 5. AGR2 co-localizes with MUC1 *in vivo*

(A) Co-immunofluorescence in a *Pdx1-Cre/Kras*^{G12D}*/p53*$^{L/L}$ model. Shown are mouse low-grade PanIN lesions stained for AGR2 (red), MUC1 (green), and DAPI (blue). The merged image from AGR2 and MUC1 is shown in the far right panel. Yellow color indicates areas of co-localization of AGR2 and MUC1. Magnification: 100×; Scale bar: 40 μm. **(B)** Alcian blue staining combined with immunohistochemical detection of AGR2 in mPanIN-3 and early invasive adenocarcinoma from a *Pdx1-Cre/Kras*^{G12D}*/Smad4*$^{L/L}$ model. Magnification: 200×; Scale bar: 20 μm. **(C)** Immunohistochemistry of AGR2 (left) and MUC1 (right) in serial sections of human pancreas, with the same area of the mPanIN structure magnified in an enlarged view. An mPanIN-2 lesion is seen on the left, within a larger area of ADM. Early adenocarcinoma shown on the right, and is enlarged in the box. Invasive clusters surround the larger lesion and stain highly for AGR2. Magnification: 100×; Scale bar: 40 μm.

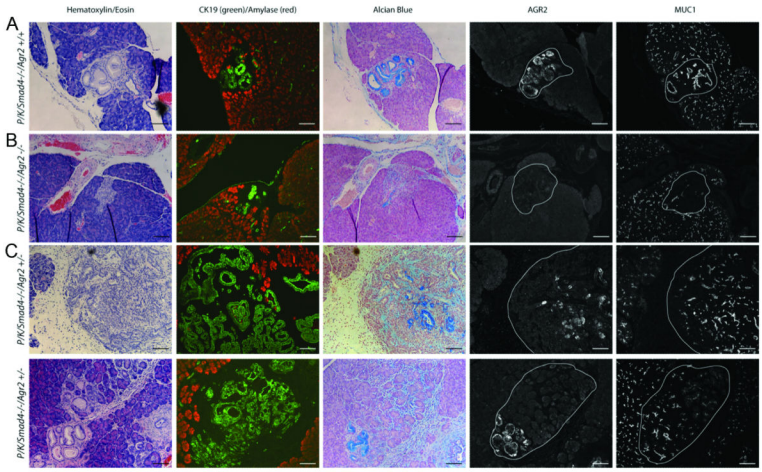

Figure 6. AGR2 is required for MUC1 expression *in vivo*

This figure shows serial sections of the same lesion, stained with either hematoxylin/eosin (column 1), co-IF for CK19 and amylase (column 2), Alcian blue (column 3), IF for AGR2 (column 4), or IF for MUC1 (column 5). **(A)** An mPanIN-1 lesion from *Pdx1-Cre/Kras^{G12D}/Smad4$^{L/L}$* (AGR2 positive**)**. **(B)** An mPanIN-1 lesion from *Pdx1-Cre/Kras^{G12D}/Smad4$^{L/L}$/Agr2$^{-/-}$* (AGR2 negative). **(C)** Low-grade adenocarcinoma from *Pdx1-Cre/Kras^{G12D}/Smad4$^{L/L}$/Agr2$^{+/-}$* (AGR2 heterogeneous). **(D)** mPanIN-1/PanIN-2 lesion from *Pdx1-Cre/Kras^{G12D}/Smad4$^{L/L}$/Agr2$^{+/-}$* (AGR2 heterogenous). Magnification: 100×; Scale bar: 40 μm.

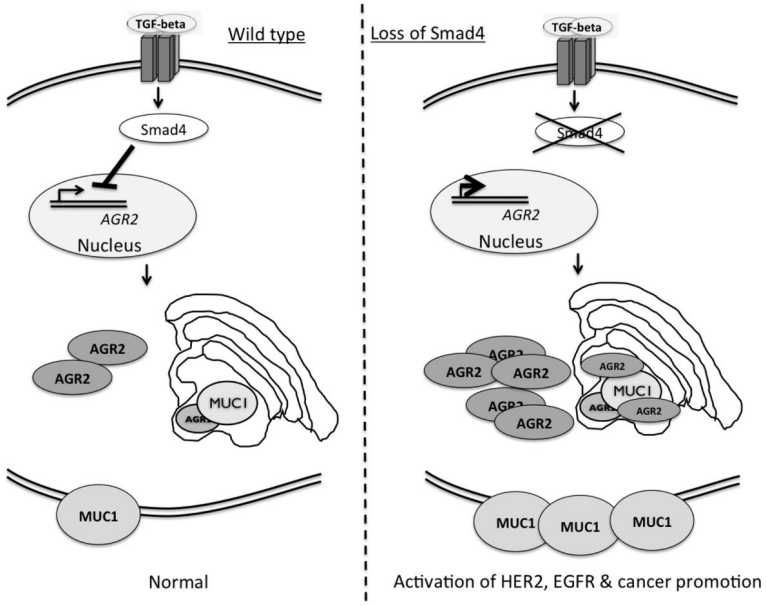

Figure 7. Model of AGR2 regulation by TGF-β and its involvement with MUC1 in pancreatic cancer cells

We describe a model in which, through one of potentially many mechanisms, AGR2 is negatively regulated by TGF-β signaling. In the presence of TGF-β, SMAD4 translocates to the nucleus, binds to SMAD-binding elements, and interacts with nuclear effectors of transcription. In the case of *AGR2*, SMAD4 facilitates a repression of *AGR2* transcription and prevents its downstream stabilization of MUC1 in the endoplasmic reticulum.

Oncogene. Author manuscript; available in PMC 2014 February 15.

Table 1

Pathological characterization of pancreatic disease in *Pdx1-Cre/LSLKras$^{G12D/+}$/Smad4$^{lox/lox}$* mice lacking none, one or both copies of *Agr2*

Gt	#	ADM	P-1	P-2	P-3	PDAC	mm tumor	cysts
P/K/S$^{L/L}$	1							
	2	×	×	×		×	1	
	3							
	4		×					×
	5	×	×					×
	6	×						
	7					early		
	8	×	×	×	×	×	2	×
	9	×	×	×		×	15	
	10		×					
	11		×			×	8	
	12		×	×		×	3	×
	13	×	×					
	14	×	×	×	×	×	1	×
P/K/S$^{L/L}$/A$^{+/-}$	1							
	2	×	×	×				
	3					early		
	4							
	5		×	×	×	early		
	6	×	×	×		early		
	7		×			×	3	
	8							×
	9							
	10	×	×	×	×	early		
	11			×		early		
	12							

Gt	#	ADM	P-1	P-2	P-3	PDAC	mm tumor	cysts
	13							
	14							
	15	×	×					
P/K/$S^{L/L}$/$A^{-/-}$	1							
	2							
	3		×			early		

Definitions: Gt = genotype; ADM = acinar-to-ductal metaplasia; P-1 = mouse pancreatic intraepithelial neoplasia (mPanIN)1; P-2 = mPanIN2; P-3 = mPanIN3; PDAC = pancreatic ductal adenocarcinoma; mm tumor = widest measurement, in mm, of PDAC; "×" indicates the presence of; $PKS^{L/L}$ = *Pdx1-Cre/LSLKras$^{G12D/+}$/Smad4$^{lox/lox}$*; $PKS^{L/L}A^{+/-}$ = *Pdx1-Cre/LSL-Kras$^{G12D/+}$/Smad4$^{lox/lox}$/Agr2$^{+/-}$*; $PKS^{L/L}A^{-/-}$ = *Pdx1-Cre/LSL-Kras$^{G12D/+}$/Smad4$^{lox/lox}$/Agr2$^{-/-}$*